First-principles calculation of positron annihilation characteristics at metal vacancies

T. Korhonen, M. J. Puska, and R. M. Nieminen
Laboratory of Physics, Helsinki University of Technology, FIN-02150 Espoo, Finland
(Received 2 May 1996)

Annihilation characteristics for positrons trapped at metal vacancies are calculated from first principles. The calculations are based on different implementations of the two-component density-functional theory, and different numerical methods to solve the ensuing Kohn-Sham equations have been employed. The convergence of the positron annihilation characteristics calculated within different schemes is discussed, and the positron lifetimes obtained are compared with experiment. [S0163-1829(96)07145-7]

I. INTRODUCTION

The experimental methods based on positron annihilation provide a powerful tool for investigating vacancy-type defects in solids.[1] The methods are based on the trapping of positrons at open volume defects in which the positron lifetime increases compared to the bulk lifetime due to a reduced positron-electron overlap. Because of the high trapping probability, the experimental methods are sensitive to defects already at low defect ($\sim 10^{-6}$) concentrations. However, the measured data are indirect, and therefore the proper interpretation of experimental results requires theoretical calculations for the positron annihilation characteristics. The theoretical results, in turn, should be as reliable and consistent as possible. The theoretical scheme should produce positron bulk lifetimes in agreement with experiments and the bulk and vacancy lifetimes should be converged with respect to the numerical methods used.

There have been several theoretical studies of positron annihilation characteristics for defects in solids. Usually, the focus of a study has been certain defect species in a certain material. The calculations have been performed usually within one theoretical scheme describing the electron-positron system and by one method for the numerical solution of the problem. Our aim in this work is to address different ''first-principles'' schemes for describing positron states and annihilation characteristics for defects in solids. All these schemes correspond to different approximations within the two-component density functional theory (TCDFT).[2] The results obtained are valuable guidelines when constructing theories for the electron-positron interactions (e.g., for the electron-positron correlation effects in the case of a positron trapped by a vacancy). In order to attain conclusive results, the parameters calculated should be numerically stable against different approximations *within* a given computational method. Moreover, a convergence *between* different numerical methods should be reached. Recently, there have been a few calculations for positron states at vacancies in semiconductors employing state-of-the-art electronic-structure methods and the TCDFT.[3–5] In this work our aim is to raise the status of the calculations of the positron annihilation characteristics for metals and to provide calculated benchmarks for positron lifetimes at vacancies in metals.

In this paper, we present results of first-principles density-functional calculations for the positron states and annihilation characteristics for vacancies in four fcc (Al, Cu, Ag, Au) and two bcc (Fe, Nb) metals. We employ the supercell approach; i.e., instead of a single isolated vacancy in an infinite lattice our system consists of a periodic array of vacancies with a certain size of the (super)cell. There has been some discussion on the convergence of the results with respect to the supercell size in the case of metals,[6] metal carbides and nitrides,[7] and compound semiconductors,[8] but there has not yet been a systematic study of the effects of periodic boundary conditions used in the calculation for the positron state. One of the main results of the present work is to show a practical way how positron annihilation characteristics independent of the size of the supercell can be reached. The organization of the present paper is as follows. In Sec. II, the computational models, i.e., different schemes to describe the electron-positron correlation effects, are presented. Section III contains information on different calculational schemes used to solve the Kohn-Sham equations and it also includes the details of the computations. Section IV contains the results obtained and the discussion. Section V is a short summary.

II. MODELS

The calculation of the positron states and the annihilation characteristics is based on the density functional theory[9] (DFT) and its generalization to treat two-component systems (TCDFT).[2] In the latter the basic variables are the (average) electron and positron densities $n_e(\mathbf{r})$ and $n_p(\mathbf{r})$, respectively.

In the case of a delocalized positron in a perfect lattice, the positron density is everywhere vanishingly small. Then the positron density does not affect the average bulk electronic structure and the effective potential for the electrons has the same form as in the normal one-component formalism. We use the local density approximation (LDA) for the electron exchange-correlation effects and write

$$V_e^{\mathrm{eff}}(\mathbf{r}) = -\phi[\{Z_I,\mathbf{R}_I\},n_e] + v_{\mathrm{xc}}(n_e(\mathbf{r})), \tag{1}$$

where $\phi[\{Z_I,\mathbf{R}_I\},n_e(\mathbf{r})]$ is the Coulomb potential due to nuclei (charges Z_I and positions $\mathbf{R}_I$) and electron density n_e. v_{xc} is the LDA exchange-correlation potential for a pure electronic system. In practice, we use for the exchange-correlation energy the form suggested by Perdew and Zunger[10] to interpolate between the results by Ceperley and

Alder[11] for the homogeneous electron gas. The electron density is thus solved self-consistently without the positron. Then the effective positron potential is constructed as

$$V_p^{\mathrm{eff}}(\mathbf{r}) = +\phi[\{Z_I,\mathbf{R}_I\},n_e] + V_{\mathrm{corr}}(\mathbf{r}), \tag{2}$$

where the correlation potential V_{corr} is the the functional derivative of the electron-positron correlation energy $E_{\mathrm{corr}}[n_e,n_p]$ with respect to the positron density. In the limit of the vanishing positron density the electron-positron correlation energy does not depend on n_p. Thus one can solve for the positron wave function without any self-consistency iterations for the positron state. The electron-positron correlation energy is calculated using the LDA as

$$E_{\mathrm{corr}}[n_e,n_p] = \int d\mathbf{r} n_p(\mathbf{r})\epsilon_c(n_e(\mathbf{r})), \tag{3}$$

where ϵ_c is the correlation energy for a delocalized positron in a homogeneous electron gas. The correlation potential $V_{\mathrm{corr}}(\mathbf{r})$ is seen to be equal to $\epsilon_c(n_e(\mathbf{r}))$. For the correlation energy ϵ_c we have used the parametrization introduced by Boroński and Nieminen[2] based on the homogeneous electron gas results calculated by Arponen and Pajanne.[12]

The positron lifetime τ is calculated as the inverse of the positron annihilation rate λ. In the limit of the vanishing positron density the LDA gives

$$\lambda = \pi r_e^2 c \int d\mathbf{r} n_p(\mathbf{r}) n_e(\mathbf{r}) g_0(n_e(\mathbf{r})), \tag{4}$$

where r_e is the classical electron radius and c is the speed of light. g_0 is the enhancement factor, i.e., the contact value of the electron-positron pair-correlation function, taking into account the short-range pileup of electrons at the positron. We have used the enhancement factor fitted by Puska *et al.*[4] to Lantto's[13] data quoted by Boroński and Nieminen.[2] This enhancement factor is very close to the fit of Ref. 2 and it is the zero-positron-density limit of a LDA fit to the enhancement factor in a two-component system.

The LDA for the enhancement factor has been shown to lead to too short positron lifetimes compared to the experiment.[14] In order to improve the agreement between theory and experiment Barbiellini *et al.*[14] have introduced a generalized gradient approximation (GGA) in which the enhancement factor in a given point depends both on the electron density and its gradient at that point. It has been found[15] that the ratio between the experimental and the LDA lifetimes is nearly constant for a wide range of materials. Therefore, a simple scaling would correct the LDA lifetimes to agree well with experiments. Furthermore, for this reason the LDA should predict the ratio of the positron lifetimes for two different systems (such as a perfect bulk and a vacancy) better than the absolute values of the lifetimes. The lifetime ratios between the vacancy and bulk systems calculated within the LDA and the GGA are very similar as will be shortly demonstrated below. The extension to the TCDFT is straightforward only in the LDA. For these reasons we use in the systematic comparisons of this work the LDA enhancement factor fitted in Ref. 4.

In the case of a positron trapped by a vacancy the positron density at the defect is of the same order as the local electron density. Then one should use the TCDFT and solve simultaneously and self-consistently for the mutually interacting electron and positron densities. We have used the two-component LDA scheme suggested by Boroński and Nieminen[2] for the electron-positron correlation energy. In this scheme the correlation energy functional depends on both the electron and the positron densities. The effective potential for the electrons reads

$$V_e^{\mathrm{eff}}(\mathbf{r}) = -\phi[\{Z_I,\mathbf{R}_I\},n_e,n_p] + v_{\mathrm{xc}}(n_e(\mathbf{r})) + \frac{\delta}{\delta n_e}E_{\mathrm{corr}}[n_e,n_p], \tag{5}$$

and the effective positron potential is

$$V_p^{\mathrm{eff}}(\mathbf{r}) = +\phi[\{Z_I,\mathbf{R}_I\},n_e] + \frac{\delta}{\delta n_p}E_{\mathrm{corr}}[n_e,n_p]. \tag{6}$$

Note that a self-interaction correction has been made in the positron potential (2): The Coulomb potential does not depend on the positron density and there is no exchange-correlation potential depending on the positron density. The positron annihilation rate is calculated as

$$\lambda = \pi r_e^2 c \int d\mathbf{r} n_p(\mathbf{r}) n_e(\mathbf{r}) g(n_e(\mathbf{r}),n_p(\mathbf{r})), \tag{7}$$

where the enhancement factor g depends on both the electron and the positron density. In practice, we have used the two-dimensional LDA interpolation forms suggested by Puska *et al.*[4] based on Lantto's hypernetted-chain-approximation calculations[13] for the correlation energy and the enhancement factor.

We have also carried out some test calculations using the two-component model suggested by Gilgien *et al.*[3] In this model the electron-positron correlation energy is calculated in the limit of the vanishing positron density, i.e., by using Eq. (3). The electron potential [Eq. (5)] depends then on the positron density but in the positron potential [Eq. (6)] the dependence is not explicit. In this scheme the enhancement factor is calculated also in the limit of the vanishing positron density, i.e., using Eq. (4).

The schemes suggested by Boroński and Nieminen and by Gilgien *et al.* are remarkably more complicated than the procedure for a delocalized positron, where self-consistency iterations are needed only to solve for the electron density. This fact has hampered a wider use of the two-component schemes. Also the lack of a parametrization of the two-component electron-positron correlation functional has prevented the use of the scheme suggested by Boroński and Nieminen. Only recently have there appeared a few calculations using the full TCDFT.[3,4,16] Instead of the two-component schemes the so-called conventional scheme has been widely used for localized positron states. In the conventional scheme localized positron states are calculated with the same procedure as the delocalized ones. The electron density is calculated without the effect of the localized positron and the positron potential and lifetime are calculated in the limit of the vanishing positron density using Eqs. (2) and (4), respectively.

III. COMPUTATIONAL METHODS

In this work, most of the calculations have been performed using the tight-binding version[17] of the linear muffin-tin orbital method within the atomic-spheres approximation (LMTO ASA).[18] In the ASA the crystal volume is divided into overlapping atom-centered spheres. The potential and the charge densities are assumed to be spherically symmetric inside each sphere. A vacancy then means an ''empty'' vacancy sphere in the crystal. The basis for one-particle (electron or positron) wave functions consist in our calculations of s, p, and d partial waves both for the metal and for the vacancy spheres. A supercell size of $N=64$ lattice sites has been used in the vacancy calculations. The Brillouin-zone integrations have been performed with the tedrahedron method[19] using an equally spaced **k**-point mesh centered around the Γ point ($\mathbf{k}=0$). When calculating the positron states the energy linearization parameters E_ν's have been iterated until they are equal to the positron eigenvalue. Both the full two-component schemes and the conventional scheme have been employed.

The LMTO ASA is known to work quite well for electron states in metals, for which the atomic packings are dense. The spherical approximation is correct close to nuclei, where most of the electron density resides. The situation for the positron is different. Due to the strong repulsion between the positron and the positive ion cores, the positron density is peaked in the interstitial regions. There the spherical approximation is not adequate. In order to check the effects of the ASA we have used also the full-potential linear muffin-tin orbital (FP-LMTO) method,[20,21] which makes no shape approximation to the potential or to the charge densities. The electron wave functions are presented in these calculations with the basis consisting of s, p, and d partial waves with kinetic energies of $-\kappa=-0.01$ Ry and -1.0 Ry. The partial waves are centered around the ideal lattice sites. Thus 18 functions per sphere have been used. The densities and potentials are expanded in spherical harmonics up to an angular momentum of $l_{\max}=4$. The vacancy is modeled by a supercell containing 27 lattice sites both for the fcc and bcc metals. The **k**-space integrations have been performed with special point meshes of ten and eight irreducible points for the bcc and fcc supercells, respectively. For a better numerical stability, each energy sampled has been broadened with a Gaussian, having a width of $\sigma=20$ mRy. The positron calculations have been performed within the conventional scheme.

We have used also the so-called atomic superposition (AT-SUP) method[22] in order to calculate positron lifetimes without any geometrical shape approximations. The method employs non-self-consistent electronic structures obtained by superimposing free-atom densities. For a given system, the electron density and the positron potential are constructed on the points of a real-space mesh using the conventional scheme. The resulting three-dimensional Schrödinger equation for the positron state is solved in a real-space point mesh[23] which is used also to calculate the positron annihilation rate. The AT-SUP method is computationally very effective when compared to the methods using self-consistent electron densities. For example, we have treated vacancies in the AT-SUP method with supercells containing up to 256 and 250 lattice sites in the fcc and bcc structures, respectively.

In all the above methods the delocalized positron states in perfect bulk lattices are calculated at the Γ point. This is the appropriate state for a thermalized positron because the energy of the lowest-lying positron state increases very rapidly when moving away from the Γ point (the positron band mass is only slightly larger than the free positron mass).

In the supercell approximation an isolated vacancy is replaced by a periodic vacancy structure. If the supercell is large enough, the vacancies do not interact with each other and the situation describes well an isolated vacancy. However, in practice the supercell size cannot be made arbitrarily large. As a result, the vacancies can be quite close to each other and there are residual interactions between the vacancies. In the case of positron states, the energy eigenvalue corresponding to an isolated vacancy is broadened to a narrow band of energies. The lowest-energy state in the (artificial) vacancy lattice corresponds to the Γ point. In this state the derivative of the positron wave function vanishes at the cell boundaries between adjacent vacancies. If the positron density is normalized to one positron inside the supercell, the positron density corresponding to the Γ point is at the cell boundaries larger than it would be at the same distance from an isolated vacancy. Consequently, the density at center of the vacancy in a vacancy array is lower than that for an isolated vacancy. Another (natural) possibility when calculating the positron state in the vacancy superlattice is to require that the positron wave function vanish at the cell boundary. This means that the state is calculated for the top of the energy band at a **k** point which lies on the surface of the Brillouin zone. This leads to too low a positron density at the cell boundary and to too large a density at the center of the vacancy compared to an isolated vacancy. The above facts suggest that one should calculate the positron density by sampling over several **k** points in the Brillouin zone. Equivalently, one should calculate the positron density by filling the lowest (nearly dispersionless) positron band and by integrating over the Brillouin zone. The necessity to use several **k** points instead of the Γ point only has also been demonstrated in the electronic-structure calculations of defects in semiconductors[24] and in metals.[25]

The Brillouin-zone integration for the lowest positron band in the vacancy superlattice is easy to perform in the electron-band-structure codes such as the LMTO methods. In the case of the AT-SUP method the (complex) positron wave functions corresponding to different **k** points can be easily obtained by applying in the real-space grid *the boundary conditions* given by the Bloch theorem for the supercell. This is maybe a simpler way than the explicit use of *the Bloch wave functions* introduced by Ishibashi[26] for positron sates at different **k** points. The efficiency of the Brillouin-zone integration to accelerate the convergence of the positron properties as a function of the supercell size is demonstrated in Figs. 1 and 2. Figure 1 gives the positron density at a copper vacancy treated with the supercell approach and the real-space AT-SUP method. The positron density calculated with the supercell of $N=256$ atomic sites for the Γ point can be considered as well converged close to that for an isolated vacancy. This density is seen to be bracketed with the positron densities calculated with a supercell with $N=32$ atomic

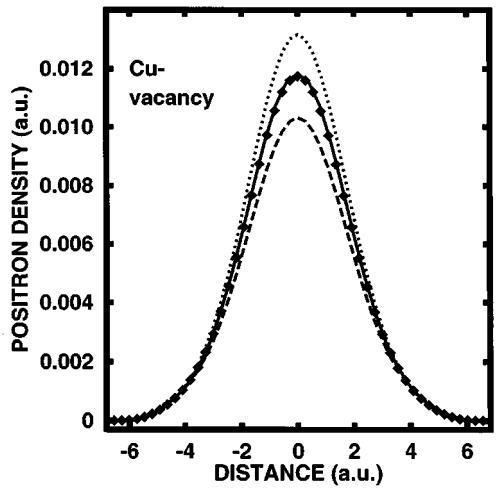

FIG. 1. Positron density at the Cu vacancy. The density is given along a line in the [100] direction and passing through the center of the vacancy. The AT-SUP method has been used. The solid line corresponds to a Γ-point calculation with a supercell size of $N=256$ lattice sites, the dashed line to a Γ point, and the dotted line to a **k** point on the Brillouin-zone surface with a supercell size of $N=32$. The markers are the average of results corresponding the two **k** points and $N=32$.

sites and corresponding to the two above-mentioned **k** points. The effect of the boundary conditions is seen to be large in the $N=32$ case. Finally, the Brillouin-zone integration for the $N=32$ supercell, which is equivalent to calculating the average of the two densities, gives a distribution very close to that obtained with the $N=256$ supercell. Figure 2 gives the positron lifetime calculated from the densities corresponding to the two **k** points and to the average density as a function of the supercell size. The results obtained with one **k** point converge rather slowly but the use of the Brillouin-zone integration leads to a rapid convergence.

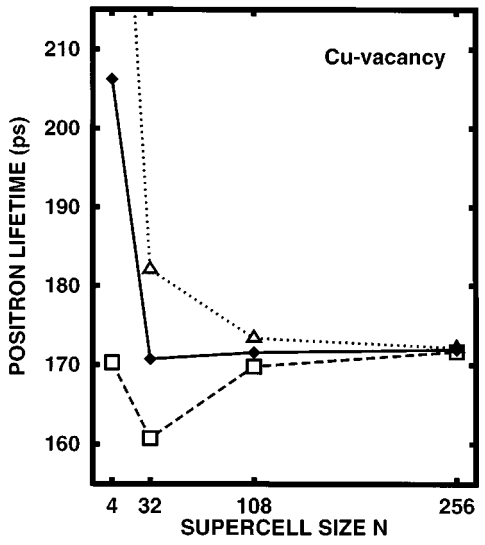

FIG. 2. Calculated positron lifetimes for the Cu vacancy as a function of the supercell size N. The AT-SUP method has been used. The dashed line corresponds to the Γ-point calculations, the dotted line to a **k** point on the Brillouin-zone surface calculations, and the solid line to the Brillouin-zone integration calculations; i.e., the average of the Γ point and a **k** point on the Brillouin-zone surface densities is used.

TABLE I. Calculated and experimental positron lifetimes for bulk metals. All lifetimes are in ps.

Method	Cu fcc	Ag fcc	Au fcc	Al fcc	Fe bcc	Nb bcc
LMTO-ASA	105	120	107	165	100	120
FP-LMTO	106	122	109	168	99	121
AT-SUP	109	124	112	170	102	127
Experiment	110 [a]	131 [a]	117 [a]	163 [a]	106 [a]	119 [a]
		120 [b]			170 [b]	112 [b]

[a]Reference 35.
[b]Reference 36.

IV. RESULTS AND DISCUSSION

The positron lifetimes calculated in this work for bulk metals are given in Table I together with experimental data. The scatter in the experimental bulk data is seen to be up to 10 ps. It is expected that the experimental positron lifetimes at vacancies show similar error bars but that the ratios between the vacancy and bulk lifetimes from the same series of measurements should be more accurate. The theoretical results are obtained by the AT-SUP, LMTO-ASA, and FP-LMTO methods. In all calculations the experimental lattice constants quoted in Ref. 27 have been used. With the exception of Al and Nb, the theoretical values are shorter than the experimental ones. The use of a LDA interpolation form based on the many-body calculations by Arponen and Pajanne[12] leads to lifetimes consistently shorter than the experimental ones and the corresponding GGA would then improve the agreement.[14,15] The LMTO-ASA and FP-LMTO methods, which use self-consistent electronic structures, give almost the same lifetimes. Therefore the ASA seems to work quite well for the positron in bulk metals, as it does for the electrons. The differences between the positron lifetimes calculated with the AT-SUP method and either of the LMTO methods are on the average somewhat larger than the differences between the two LMTO methods. Thus for these positron bulk lifetimes the self-consistency of the electronic structure seems to be more important than the shape approximations.

Figures 3(a) and 3(b) show the electron and positron densities at Cu and Nb vacancies along the lines in the [110] and [111] directions, respectively. The densities displayed include those calculated using the LMTO-ASA method and the conventional and both two-component schemes for the electron-positron interaction. These three-dimensional densities correspond to spherical potentials in the atomic and vacancy spheres, i.e., they are not the spherically averaged densities used in the self-consistent calculations. The FP-LMTO results, which are obtained without shape approximations in the potential and within the conventional scheme, are also given. The localized positron is seen to raise the electron density inside the vacancy in the scheme suggested by Boroński and Nieminen from that of the clean vacancy, i.e., from the electron density in the conventional scheme, whereas the positron densities are almost

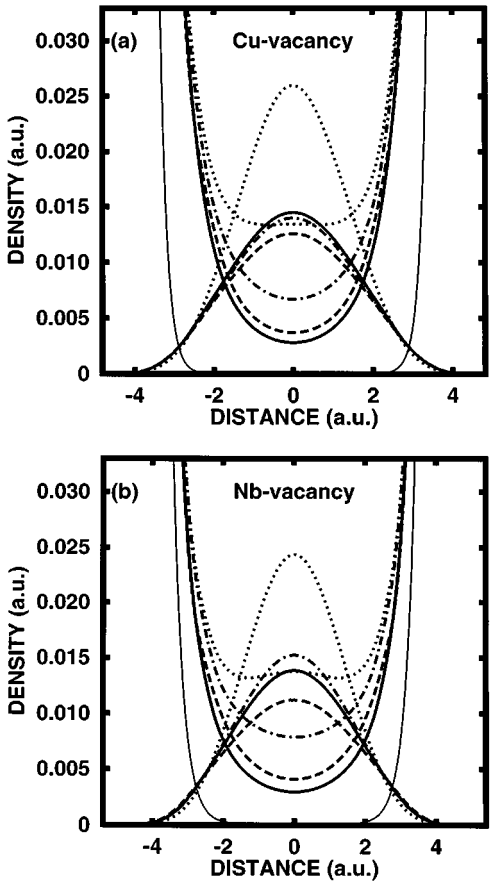

FIG. 3. Positron and electron densities at (a) the Cu and (b) the Nb vacancy. The densities are given along a line in the [110] ([111]) direction and passing through the center of the Cu (Nb) vacancy. Shown are the results of the schemes suggested by Boroński and Nieminen (dot-dashed line), by Gilgien *et al.* (dotted line), and conventional scheme (solid line) calculated by the LMTO-ASA method and those of the conventional scheme calculated by the FP-LMTO method (dashed line). The core electron densities calculated by the LMTO-ASA method are also shown in the figures (thin solid lines).

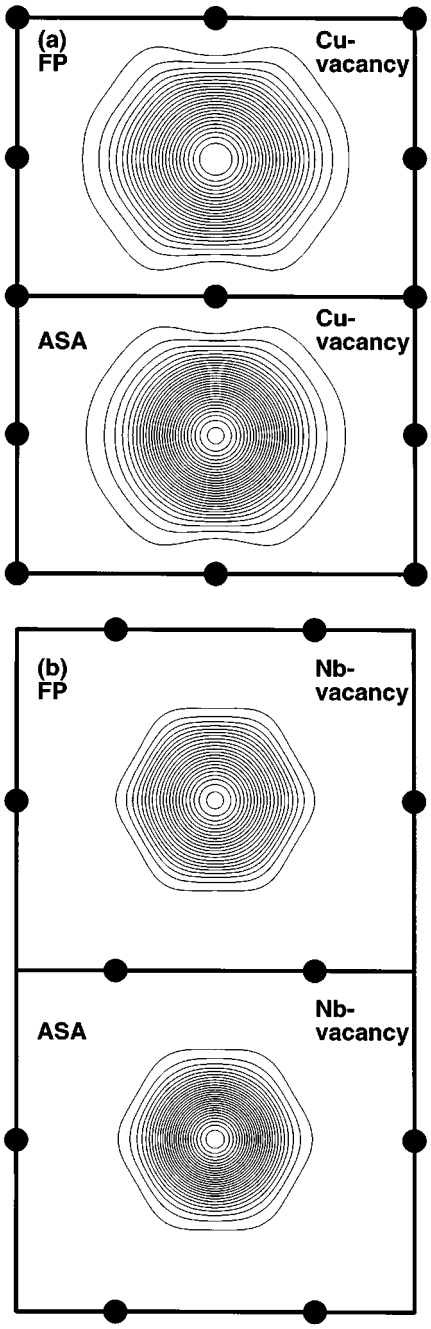

FIG. 4. Positron density at (a) the Cu and (b) the Nb vacancy calculated using the FP-LMTO and LMTO-ASA methods. The densities are shown on the (110) and (111) planes for the Cu and Nb vacancies, respectively. The spacing between the contour lines is 0.0005 a.u.

identical. The method suggested by Gilgien *et al.* is seen to localize the positron very strongly to the vacancy, and the electron density is also increased due to the direct Hartree interaction between the positron and the electrons. The FP-LMTO calculation gives a slightly larger electron density and a slightly smaller positron density in the vacancy than the ASA calculation. The shapes of the densities are very similar, which is seen from Figs. 4(a) and 4(b), which show the calculated positron densities at Cu and Nb vacancies on the (110) and (111) planes, respectively.

The behaviors of the electron and positron densities in the 2 two-component schemes and in the conventional scheme support the ideas found in the earlier calculations for a positron trapped by the Ga vacancy in GaAs.[4] The fact that the model suggested by Gilgien *et al.* leads to more localized positron states at defects than the model suggested by Boroński and Nieminen reflects the stronger electron-positron correlation potential for positrons in the former model. In the latter model the two-component correlation potential decreases as the positron density increases whereas in the former one it has its maximum strength corresponding to the limit of the vanishing positron density. The similarity of the positron density obtained in the scheme suggested by Boroński and Nieminen compared to the conventional scheme can be explained as follows: The correlation potential in the scheme by Boroński and Nieminen decreases when the positron density increases and this opposes the lowering of the Hartree part due to the positron-induced increase in the electron density at the defect.

Figure 5 shows the positron lifetimes as a function of the supercell size for Cu (fcc) and Nb (bcc) vacancies as calcu-

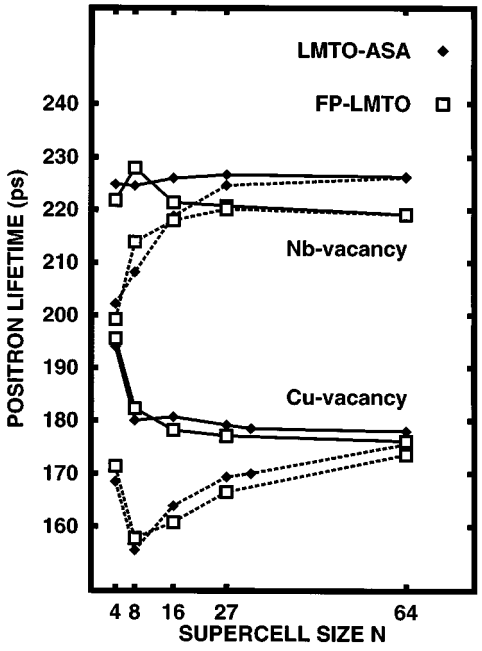

FIG. 5. Calculated positron lifetimes for the Cu and Nb vacancies as a function of the supercell size N. The LMTO-ASA and FP-LMTO methods have been used together with the conventional scheme. The solid lines correspond to the calculations with the Brillouin-zone integrations and the dashed lines to the Γ-point calculations.

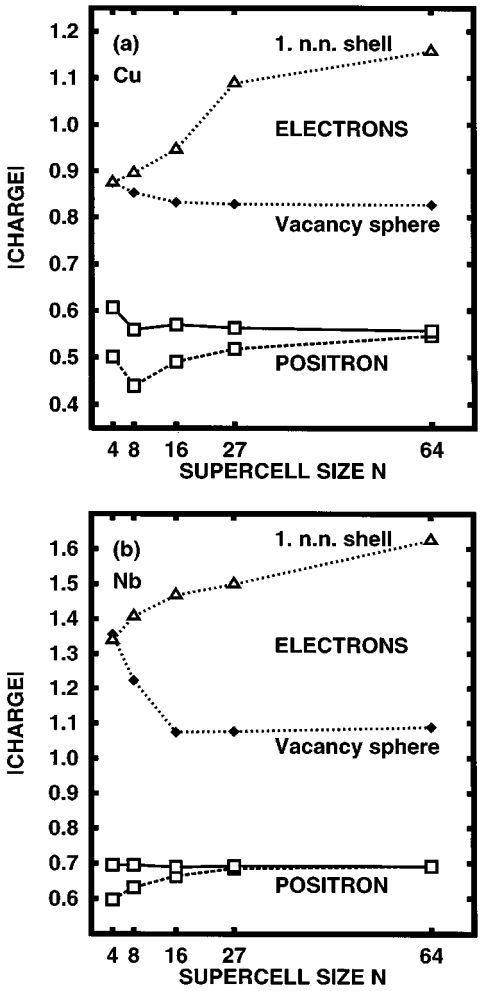

FIG. 6. Integrated electron (solid diamonds) and positron (open squares) charges inside the vacancy sphere and the difference between the nuclear charge and the total number of electrons for the nearest-neighbor shell (open triangles) as a function of the supercell size N for (a) Cu and (b) Nb . The LMTO-ASA method in the conventional scheme has been used. For the electrons the solid (open) markers correspond to a net negative (positive) charge. For the positron the solid line corresponds to the Brillouin-zone integration calculations for positron and the dashed line to the Γ-point ones.

lated by the LMTO-ASA and the FP-LMTO methods. The conventional scheme has been used. In calculations employing only the Γ point for the positron density the convergence as a function of the supercell size is rather slow. The calculation of the positron density by integrating over the lowest-lying positron band in the Brillouin zone gives a much faster convergence. The variations in the positron lifetime are mainly a positron state effect. The electronic structure inside the vacancy converges quite rapidly because of the very efficient electronic screening in metals.[28] This can be seen from Fig. 6, in which the difference between the total number of electrons and the nuclear charge is plotted as a function of the supercell size for the vacancy sphere and for the nearest-neighbor atomic shell. The convergence of the electron charge for the vacancy sphere is achieved already around $N=16$. The development of the total positron charge inside the vacancy sphere is also given, and it shows that the Brillouin-zone integration gives the correct positron number much before the simple Γ-point calculation. The importance of the development of the positron state is clear also from the similarity of the Γ-point results for the Cu vacancy in Figs. 5 and 2. The latter are obtained by the AT-SUP method, in which one only adds more neutral atoms around the vacancy to increase the supercell size. Therefore the electron density around the vacancy converges in the AT-SUP method due to the lack of the charge transfer very rapidly to the bulk density.

In order to study the benefits of the rapid convergence of the electron density we have calculated the positron state and lifetime for the Cu vacancy by starting from the LMTO-ASA results with small supercells of $N=27$ or $N=16$, and extending these to $N=64$ in a non-self-consistent manner by adding spheres corresponding to the bulk Cu. The positron lifetimes obtained in the conventional scheme, 180 ps and 181 ps, respectively, are close to the result of 178 ps calculated using the self-consistent electronic structure of an $N=64$ supercell. Thus the $N=27$ and even the $N=16$ supercells should be large enough to calculate the positron lifetimes to a reasonable accuracy in ideal metal vacancies. On the other hand, in the 2 two-component schemes it is better use a larger supercell, e.g., that of an $N=64$. This is because in order to make the Coulomb potential finite one has to neutralize the positron charge by adding a compensating (constant) negative background charge to the supercell. In order to make the induced errors as small as possible, one has to use a supercell as large as computationally reasonable.

The positron lifetimes calculated for the vacancies in dif-

TABLE II. Calculated and experimental positron lifetimes for metal vacancies. Also shown are the ratios τ_v/τ_b of the vacancy lifetimes τ_v to the corresponding bulk lifetimes τ_b. Shown are the results of the two-component scheme suggested by Boroński and Nieminen calculated by the LMTO-ASA method, and the conventional scheme results calculated by the LMTO-ASA, FP-LMTO, and AT-SUP methods. The vacancy has been modeled by a supercell containing $N=27$ and $N=64$ lattice sites in the FP-LMTO and LMTO-ASA calculations, respectively. In the AT-SUP calculations $N=54$ and $N=108$ lattice sites has been used for the bcc and fcc metals, respectively. The experimental lifetimes for Cu, Ag, Au, Al, Fe, and Nb are from Refs. 37, 38, 39, 40, 41, and 42, respectively. The values in parentheses on the last line are calculated using the experimental bulk lifetimes from Table I instead of the values found in the same references as the experimental vacancy lifetime data.

Method		Cu fcc	Ag fcc	Au fcc	Al fcc	Fe bcc	Nb bcc
LMTO-ASA, two-component							
τ_v	(ps)	176	209	207	260	181	236
(τ_v/τ_b)		1.68	1.75	1.93	1.57	1.81	1.96
LMTO-ASA							
τ_v	(ps)	178	210	206	250	179	226
(τ_v/τ_b)		1.70	1.76	1.92	1.51	1.80	1.88
FP-LMTO							
τ_v	(ps)	177	208	204	246	182	221
(τ_v/τ_b)		1.67	1.71	1.88	1.47	1.85	1.82
AT-SUP							
τ_v	(ps)	172	201	192	248	178	225
(τ_v/τ_b)		1.58	1.62	1.71	1.46	1.75	1.77
Experiment							
τ_v	(ps)	179	198	210	251	175	210
(τ_v/τ_b)		1.63	1.41	1.68	1.54	1.59	1.72
(τ_v/τ_b)		(1.63)	(1.51)	(1.79)	(1.54)	(1.65)	(1.76)

ferent fcc and bcc metals are given in Table II. The scheme suggested by Boroński and Nieminen has been applied using the LMTO-ASA method. These results can be compared with the corresponding conventional scheme results. Moreover, the positron lifetimes obtained by the LMTO-ASA, FP-LMTO, and AT-SUP methods are compared within the conventional scheme. The results of both schemes are, maybe with the execption of Al and Nb, rather close to each other. The annihilation rate increases in the two-component scheme due to the increased electron-positron overlap but this increase is compensated by the decrease of the enhancement factor as the positron density increases leading to similar results as in the conventional scheme.[4] The different computational methods give in the conventional scheme positron lifetimes within few ps from each other. The LMTO-ASA and the FP-LMTO results are on the average closer to each other than to the AT-SUP results. This indicates the importance of the self-consistent electronic structure. All the theoretical estimates for the positron lifetimes are in a fair agreement with the experimental results given in Table II.

Our test calculations using the scheme suggested by Gilgien *et al.* show that the strong localization of the positron density at the vacancy tends to increase the positron lifetime, but the use of the zero-positron-density limit for the enhancement factor in this scheme shortens it. The effects have a tendency to cancel each other and the positron lifetime is close to the value obtained in the scheme suggested by Boroński and Nieminen.

In order to compare more clearly the results obtained by different calculation methods with each other and with the experimental ones we show in Table II the ratios τ_v/τ_b between the vacancy and bulk lifetimes. These ratios are not very sensitive to the enhancement factor used.[15] For example, the positron lifetimes obtained for the vacancy in Cu within the conventional LDA and GGA schemes using LMTO-ASA method are 178 and 193 ps, respectively. The τ_v/τ_b ratios are in a better agreement; i.e., they are 1.70 and 1.63, respectively. Also systematic experimental errors are expected partly to cancel in the ratios between the vacancy and bulk lifetimes. The AT-SUP method gives the lowest τ_v/τ_b ratios. The use of self-consistent electronic structures in the conventional scheme increases the ratios, whereas the two-component and the conventional scheme used in the LMTO-ASA method give quite similar lifetime ratios (the bulk lifetimes are by definition the same in the conventional and two-component schemes when the same computational method is used). The effect of the self-consistency of the electronic structure to the τ_v/τ_b ratios is interesting. The self-consistency, i.e., the electron charge transfer relative to the density of the superimposed free atoms, increases the positron bulk lifetimes but decreases the lifetimes for vacancies.

Compared to the experimental values the τ_v/τ_b ratios calculated by the AT-SUP method are of the same order or slightly lower. The use of the self-consistent electronic structures leads, with the exception of Al, to τ_v/τ_b ratios clearly larger than the experimental ratios. This is an important feature if we consider the effects of the ionic relaxation neglected in our calculations. According to the first-principles calculations the ions neighboring the vacancy relax inwards.[25,29] The magnitude of the relaxation is around 2% of the bond length. This is a rather small relaxation compared to semiconductors, for which the open lattice structure and different possibilities of covalent bond formation give a large freedom for the ionic rearrangements around vacancies.[4,3] The small inward relaxation should shorten the positron lifetimes for metal vacancies. This can bring the positron lifetimes, or the τ_v/τ_b ratios, calculated using the self-consistent electronic structures into agreement with the experiment, but it worsens the agreement in the case of the AT-SUP method. According to the conventional scheme and two-component calculations for vacancies in semiconductors, also the positron can to some extent affect to the ionic relaxation.[4,3,30] In the case of metal vacancies this effect is expected to be smaller due to the higher atomic density. We have monitored the effects of the lattice relaxation by allowing a small relaxation of 2% inwards for ions neighboring the Cu vacancy and performing a calculation in the conventional scheme using the FP-LMTO method. The positron lifetime is shortened by 9 ps when compared to that for an ideal vacancy. The corresponding decrease in the τ_v/τ_b ratio is ~ 0.1.

The so-called core-annihilation parameter W, which can be determined, e.g., from the measurements of angular correlation of annihilation radiation or from the coincidence-Doppler line shape data,[31,32] is very sensitive to the localiza-

tion of the positron state.[33] The relative W parameter for a defect can be estimated as

$$W = \frac{(\lambda_c/\lambda)^{\text{defect}}}{(\lambda_c/\lambda)^{\text{free}}}, \tag{8}$$

where λ_c and λ are the annihilation rates with core electrons and the total annihilation rate, respectively, calculated for a positron trapped at the defect or for a free positron. The changes in the W parameter reflect changes in the relative intensity of the core annihilation and thereby the W parameter probes the positron-core-electron overlap. We have estimated the relative W parameter for the vacancy in Al by the LMTO-ASA method using the two two-component schemes and the conventional scheme. The scheme suggested by Boroński and Nieminen and the conventional scheme give the values of 0.31 and 0.37, respectively. The scheme suggested by Gilgien *et al.* gives a value of 0.14 which is clearly the smallest and reflects the strong localization of the positron wave function in this scheme. We are not aware of measurements for the relative W parameters in the case of vacancies in metals. However, Lynn *et al.*[34] have shown the ratio between two Doppler spectra measured for an Al sample close to the melting temperature and at the room temperature. At high temperatures, when the signal is expected to correspond to a high degree to the thermally generated vacancies, the ratio may sink at the relevant momenta to a value below 0.6. This is clearly less than the relative W parameters reported for monovacancies in semiconductors but remarably larger than the prediction by the scheme suggested by Gilgien *et al.*

V. CONCLUSIONS

It has been shown that *ab initio* calculations provide reliable values for the positron lifetime in metals. The calculated ratios of the lifetimes for unrelaxed vacancies and the corresponding perfect bulk lattices are usually slightly too large, but an expected slight inward relaxation of the vacancies would bring the ratios closer to the experimental values. The calculated lifetimes are seen to be quite independent of the shape approximations made in the calculations. The self-consistency of the electronic structure is found to be a somewhat more important ingredient. The so-called conventional scheme for localized positron states produces almost the same results as the more demanding full two-component calculation. A Brillouin-zone integration over the lowest-lying positron state is found to be necessary in the supercell calculations for localized positron states, in order to get a rapid convergence of the results with respect to the supercell size. Our first calculations indicate that the Brillouin-zone integration is even more important for the more delocalized positron states at vacancy-type defects in semiconductors. In practice, the conventional scheme and supercells with reasonable sizes give reliable estimates for the positron lifetime in metallic systems. This kind of positron lifetime calculation provides necessary data for the proper interpretation of the experimental data.

ACKNOWLEDGMENTS

The authors gratefully acknowledge M. Šob and J. Kuriplach for many helpful discussions and O. Jepsen for providing us with the TB-LMTO electronic structure package. This work has been made possible by generous computer resources from Center for Scientific Computing, Espoo, Finland.

[1] P. Hautojärvi and C. Corbel, in *Positron Spectroscopy of Solids*, edited by A. Dupasquier and A. P. Mills, Jr. (IOS Press, Amsterdam, 1995), p. 491.
[2] E. Boroński and R. M. Nieminen, Phys. Rev. B **34**, 3820 (1986).
[3] L. Gilgien, G. Galli, C. Gygi, and R. Car, Phys. Rev. Lett. **72**, 3214 (1994).
[4] M. J. Puska, A. P. Seitsonen, and R. M. Nieminen, Phys. Rev. B **52**, 10 947 (1995).
[5] Mineo Saito and Atsushi Oshiyama, Phys. Rev. B **53**, 7810 (1996).
[6] P. A. Sterne and J. H. Kaiser, Phys. Rev. B **43**, 13 892 (1991).
[7] M. J. Puska, M. Šob, G. Brauer, and T. Korhonen, Phys. Rev. B **49**, 10 947 (1994).
[8] F. Plazaola, A. P. Seitsonen, and M. J. Puska, J. Phys. Condens. Matter **6**, 8809 (1994).
[9] For a recent review, see R. O. Jones and O. Gunnarsson, Rev. Mod. Phys. **61**, 689 (1989).
[10] J. Perdew and A. Zunger, Phys. Rev. B **23**, 5048 (1981).
[11] D. M. Ceperley and B. J. Alder, Phys. Rev. Lett. **45**, 566 (1980).
[12] J. Arponen and E. Pajanne, Ann. Phys. (N.Y.) **121**, 343 (1979); J. Phys. F **9**, 2359 (1979).
[13] L. Lantto, Phys. Rev. B **36**, 5160 (1987).
[14] B. Barbiellini, M. J. Puska, T. Torsti, and R. M. Nieminen, Phys. Rev. B **51**, 7341 (1995).
[15] B. Barbiellini, M. J. Puska, T. Korhonen, A. Harju, T. Torsti, and R. M. Nieminen, Phys. Rev. B **53**, 16 201 (1996).
[16] Xiao-Gang Wang and Hong Zhang, J. Phys. Condens. Matter **2**, 7275 (1990).
[17] O. K. Andersen, O. Jepsen, and D. Glötzel, in *Highlight of Condensed-Matter Theory*, edited by F. Bassani, F. Fumi, and M. P. Tosi (North-Holland, New York, 1985).
[18] For a recent review, see O. K. Andersen, O. Jepsen, and M. Šob, in *Electronic Band Structure and Its Applications*, edited by M. Yussouff (Springer-Verlag, Heidelberg, 1987).
[19] O. Jepsen and O. K. Andersen, Phys. Rev. B **29**, 5965 (1984); P. Blöchl, O. Jepsen, and O. K. Andersen, *ibid.* **49**, 16 223 (1994).
[20] M. Methfessel, Phys. Rev. B **38**, 1537 (1988).
[21] M. Methfessel, C. O. Rodriguez, and O. K. Andersen, Phys. Rev. B **40**, 2009 (1989).
[22] M. J. Puska and R. M. Nieminen, J. Phys. F **13**, 333 (1983).
[23] A. P. Seitsonen, M. J. Puska, and R. M. Nieminen, Phys. Rev. B **51**, 14 057 (1995).
[24] J. Furthmüller and M. Fähnle, Phys. Rev. B **46**, 3839 (1992).
[25] N. Chetty, M. Weinert, T. S. Rahman, and J. W. Davenport, Phys. Rev. B **52**, 6313 (1995).

[26] S. Ishibashi, J. Phys. Condens. Matter **6**, L71 (1994).
[27] M. J. Puska, P. Lanki, and R. M. Nieminen, J. Phys. Condens. Matter **1**, 6081 (1989).
[28] T. Korhonen, M. J. Puska, and R. M. Nieminen, Phys. Rev. B **51**, 9526 (1995).
[29] M. J. Mehl and B. M. Klein, Physica B **172**, 211 (1992); R. Benedek, L. H. Yang, C. Woodward, and B. I. Min, Phys. Rev. B **45**, 2607 (1992).
[30] K. Laasonen, M. Alatalo, M. J. Puska, and R. M. Nieminen, J. Phys. Condens. Matter **3**, 7217 (1991).
[31] *Positrons in Solids*, edited by P. Hautojärvi, Topics in Current Physics Vol. 12 (Springer-Verlag, Heidelberg, 1979).
[32] M. Alatalo, H. Kauppinen, K. Saarinen, M. J. Puska, J. Mäkinen, P. Hautojärvi, and R. M. Nieminen, Phys. Rev. B **51**, 4176 (1995).
[33] M. Alatalo, B. Barbiellini, M. Hakala, H. Kauppinen, T. Korhonen, M. J. Puska, K. Saarinen, P. Hautojärvi, and R. M. Nieminen, Phys. Rev. B **54**, 2397 (1996).
[34] K. G. Lynn, J. E. Dickman, W. L. Brown, M. F. Robbins, and E. Bonderup, Phys. Rev. B **20**, 3566 (1979).
[35] A. Seeger, F. Barnhart, and W. Bauer, in *Positron Annihilation*, edited by L. Dorikens-Vanpraet, M. Dorikens, and D. Segers (World Scientific, Singapore, 1989), p. 275.
[36] K. Saarinen (unpublished).
[37] H. E. Schaefer, W. Stuck, F. Banhart, and W. Bauer, in *Proceedings of the 8th International Conference on Vacancies and Interstitials in Metals and Alloys*, edited by C. Ambromeit and H. Wollenberger (Trans Tech, Aedermannsdorf, Switzerland, 1986).
[38] R. H. Howell, Phys. Rev. B **24**, 1835 (1981).
[39] D. Herlac, H. Stoll, W. Trost, T. E. Jackman, K. Maier, H. E. Schaefer, and A. Seeger, Appl. Phys. **12**, 59 (1977).
[40] H. E. Schaefer, R. Gugelmeier, M. Schmolz, and A. Seeger, in *Proceedings of the Vth Risø International Symposium of Metallurgy and Materials Science*, edited by N. H. Andersen, M. Eldrup, N. Hansen, D. J. Jensen, T. Leffers, H. Lillholt, O. B. Pedersen, and B. N. Singh (Risø National Laboratory, Risø , Denmark, 1984).
[41] A. Vehanen, P. Hautojärvi, J. Johansson, and J. Yli-Kauppila, Phys. Rev. B **25**, 762 (1982).
[42] P. Hautojärvi, H. Huomo, M. Puska, and A. Vehanen, Phys. Rev. B **32**, 4326 (1985).